

CrossMark
click for updatesCite this: *RSC Adv.*, 2015, 5, 13828

Flying-seed-like liquid crystals. Part 4:† a novel series of bulky substituents inducing mesomorphism instead of using long alkyl chains

Miho Yoshioka,^a Kazuchika Ohta^{*a} and Mikio Yasutake^b

We synthesized a novel series of flying-seed-like derivatives (**3a–g**) based on phthalocyaninato copper(II) (abbreviated as PcCu) substituted by bulky groups {PhO (**a**), (*o*-C₁)PhO (**b**), (*m*-C₁)PhO (**c**), (*p*-C₁)PhO (**d**), [*m,p*-(C₁)₂]PhO (**e**), [*m,m'*-(C₁)₂]PhO (**f**), and [*m,p,m'*-(C₁)₃]PhO (**g**)} instead of using long alkyl chains, in order to investigate their mesomorphism. Their phase transition behaviour and the mesophase structures were established using a polarizing optical microscope, a differential scanning calorimeter, a thermogravimetry analyser and a temperature-dependent small angle X-ray diffractometer. It was demonstrated that (PhO)₈PcCu (**3a**) and [(*p*-C₁)PhO]₈PcCu (**3d**) show no mesophase, whereas [(*m*-C₁)PhO]₈PcCu (**3c**), {[*m,p*-(C₁)₂]PhO}₈PcCu (**3e**), {[*m,m'*-(C₁)₂]PhO}₈PcCu (**3f**), and {[*m,p,m'*-(C₁)₃]PhO}₈PcCu (**3g**) show various kinds of columnar mesophases of Col_{ro}(P2₁/a), Col_{ro}(P2₁/a), Col_{ro}(C2/m) and Col_{tet,or}, respectively, while [(*o*-C₁)PhO]₈PcCu (**3b**) shows a monotropic Col_{ro}(P2_m) mesophase. Thus, we revealed that mesomorphism could be induced by these novel bulky substituents instead of using long alkyl chains, and that the mesophase structures were greatly affected by the number and position of the methoxy groups. In particular, it is very interesting that the derivatives with methoxy group(s) at the *meta* position(s), namely, **3c**, **3e**, **3f** and **3g**, tend to show enantiotropic mesophase(s), whereas neither the derivative with no methoxy group, **3a**, nor the derivative with a methoxy group at the *para* position, **3d**, show a mesophase.

Received 30th October 2014
Accepted 23rd December 2014

DOI: 10.1039/c4ra13474e

www.rsc.org/advances

1 Introduction

Generally, liquid crystalline materials are broadly categorized into rod-like (calamitic) and disk-like (discotic) molecules from their molecular shapes. In addition to the major calamitic and discotic molecules, banana-shaped, T-shaped and the other shaped molecules are also known as minor constituents of liquid crystalline materials. Regardless of the shape, each of the liquid crystals has a flat rigid central core and several flexible long alkyl chains in the periphery in almost all the cases.¹ When the liquid crystals are heated, the peripheral long alkyl chains melt to form soft parts at first, whereas the central cores do not melt. Generally, this may induce a liquid crystalline phase (=mesophase). Hence, researchers have long believed that it is an essential requirement for a liquid crystalline molecule to have long alkyl chains in the periphery. Since the discovery of the first liquid crystals in 1888, almost all the liquid crystals

have consisted of a central rigid core and several peripheral long alkyl chains. Up to date, about 101 000 kinds of liquid crystals have been synthesized¹ and investigated in various fields, especially in liquid crystal displays.²

However, in 1911 Vorländer found unique liquid crystals that had neither a rigid core nor peripheral long alkyl chains.³ Since then though they have largely been forgotten in the past 100 years and very few research papers have reported on this type of liquid crystals.^{4–8} Fig. 1-(1) shows a representative molecular structure of sodium diphenyl acetate, Ph₂CHCOONa (**1**). In 2006, we revealed for the first time, by using temperature-dependent X-ray diffractometer, that this salt, Ph₂CHCOONa (**1**), has a hexagonal columnar (Col_h) mesophase.⁸ Its mesophase structure is depicted in Fig. 1-(1). As can be seen from this figure, the bulky substituent can freely rotate around the bond coloured in red ink to form a soft corn-shaped part instead of long alkyl chains, thus showing a columnar mesophase. In this mesophase, sodium metals form a one-dimensional nano-wire and freely rotating diphenyl acetates cover the nano-wire to form an aromatic nanotube. The mesophase-showing mechanism due to the free rotation of the bulky substituent closely resembles the flying seeds of the maple tree, so much that we named such unique liquid crystals as ‘flying-seed-like liquid crystals’.⁸

^aSmart Material Science and Technology, Interdisciplinary Graduate School of Science and Technology, Shinshu University, 1-15-1 Tokida, Ueda, 386-8567, Japan. E-mail: ko52517@shinshu-u.ac.jp; Fax: +81-268-21-5492; Tel: +81-268-21-5492

^bComprehensive Analysis Center for Science, Saitama University, 255 Shimo-okubo, Sakura-ku, Saitama 338-8570, Japan. E-mail: yasutake@apc.saitama-u.ac.jp; Tel: +81-48-858-3671

† Part 3: ref. 12 in this paper.

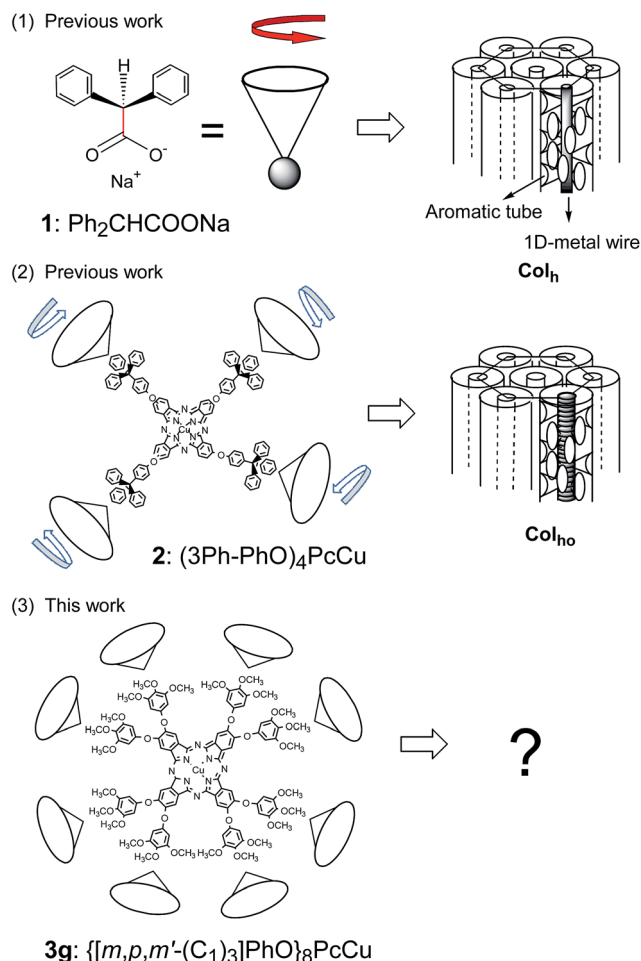


Fig. 1 Molecular and mesophase structures of flying-seed-like liquid crystals. (1) and (2) Rotating bulky substituents induced mesophases in the previous compounds.^{8,11} (3) Aim: can we induce mesophases by using novel bulky substituents? One of the bulky substituents used in this work is depicted here.

In 2009, Usolt'seva and co-workers found from polarizing optical microscopic observations that a phthalocyanine (*Pc*) derivative substituted by four triphenylmethyl groups, $(3\text{Ph-PhO})_4\text{PcCu}$ (2), as depicted in Fig. 1-(2), shows a mesophase.^{9,10} The substituent of the triphenylmethyl group in this compound very much resembles the molecular structure of $\text{Ph}_2\text{CHCOONa}$ (1) in Fig. 1-(1). Therefore, we thought that this *Pc* derivative might be one of the flying-seed-like liquid crystals induced by free rotation of the peripheral bulky substituents. In 2012, we carried out temperature-dependent X-ray diffraction studies on this *Pc* derivative 2 and revealed that it also showed a hexagonal columnar mesophase.¹¹ Furthermore, we recently reported that the introduction of the bulky substituents to the other cores also induced mesomorphism.¹²

From these investigations, we successfully established two series of bulky substituents, (i) and (ii), thereby inducing flying-seed-like liquid crystals, namely:

(i) Diphenylmethyl ($\text{Ph}_2\text{-CH-}$), 2-methylethyl ($(\text{CH}_3)_2\text{-CH-}$) and 3-ethylpropyl ($(\text{C}_2\text{H}_5)_2\text{-CH-}$).⁸

(ii) 4-(Triphenylmethyl)phenoxy (3Ph-PhO-), 4-(1,1-diphenylethyl)phenoxy (2PhO-PhO-), 4-(1-methyl-1-phenyl)phenoxy (1Ph-PhO-) and 4-(*tert*-butyl)phenoxy (0Ph-PhO-).^{11,12}

Although a very few other liquid crystals with neither a rigid central core nor flexible peripheral long alkyl chains have been reported to date,^{13–17} the mesophase-originating mechanism has never been clarified without our flying-seed-like liquid crystals.^{8,12,13} Accordingly, herein, our aim was to find a novel series of bulky substituents that could induce mesomorphism, excluding (i) and (ii), in order to further clarify how the compounds with no alkyl chains could show mesomorphism.

The previous bulky substituents of (i) and (ii) freely rotate by 360° . However, we sought to answer the question ‘when bulky substituents rotate not by 360° but flip-flop in a restricted angle region, can such bulky substituents induce mesomorphism?’ For example, Fig. 1-(3) illustrates $\{[m,p,m'-(\text{C}_1)_3]\text{PhO}\}_3\text{PcCu}$ (3g) substituted by trimethoxyphenoxy groups; can the phthalocyanine derivative show mesomorphism? In this compound, two adjacent phenoxy groups cannot freely rotate but flip-flop within the restricted angles. However, when this phenoxy group is further substituted by three methoxy groups at the *m,p,m'*-positions, the resulting bulkier substituent, $[m,p,m'-(\text{C}_1)_3]\text{PhO}$, leads to a bigger excluded volume due to the flip-flop. Accordingly, this suggests mesomorphism may be induced not only by free rotation but also by the flip-flopping of bulky substituents.

In this study, we synthesized the *PcCu* derivatives 3a–g substituted by a novel series of bulky substituent groups a–g:

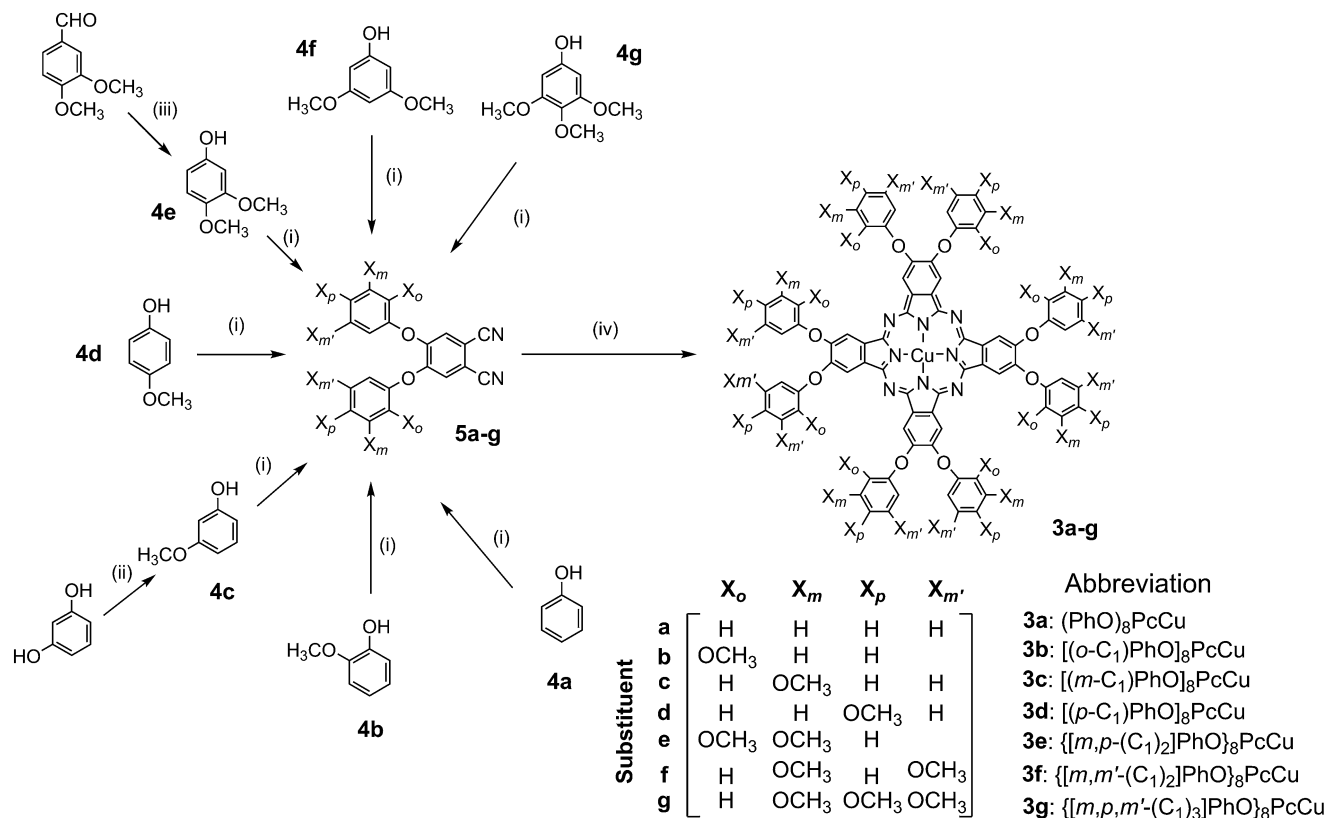
(iii) *PhO* (a); (*o*- C_1)*PhO* (b); (*m*- C_1)*PhO* (c); (*p*- C_1)*PhO* (d); $[m,p-(\text{C}_1)_2]\text{PhO}$ (e); $[m,m'-(\text{C}_1)_2]\text{PhO}$ (f); $[m,p,m'-(\text{C}_1)_3]\text{PhO}$ (g), to investigate their mesomorphism. As a result, we found that the derivatives with methoxy group(s) at the *meta* position(s) tend to show enantiotropic mesophase(s). Herein, we report the interesting results.

2 Experimental section

2.1 Synthesis

The phthalocyanine derivatives, 3a–g, were synthesized according to Scheme 1. The precursor of the phenol derivative 4c was synthesized from commercially available resorcinol (Wako) and iodomethane (Wako) using our previously reported method.¹⁸ The precursor of the phenol derivative 4e was synthesized from commercially available 3,4-dimethoxybenzaldehyde (Wako) by using our previously reported method.¹⁹ The other phenol derivatives, 4a, 4b, 4d, 4f and 4g, were purchased from Tokyo Kasei. These phenol derivatives (4a–g) were reacted with commercially available 4,5-dichlorophthalonitrile (Tokyo Kasei) to obtain the corresponding phthalonitrile derivatives (5a–g), which were converted into the corresponding phthalocyanine derivatives (3a–g).

The detailed synthetic procedures are described below only for the representative phthalocyanine derivative, $[(m-\text{C}_1)\text{PhO}]_8\text{PcCu}$ (3c). For the other precursors (5a–b and 5d–g) and for the phthalocyanine derivatives (3a–b and 3d–g), the physical property data are only described.



Scheme 1 Synthetic route for novel flying-seed-like phthalocyanines, **3a–g**. (i) 4,5-Dichlorophthalonitrile, K₂CO₃ and DMA, (ii) CH₃I, K₂CO₃ and DMF, (iii) conc. H₂SO₄, 30% H₂O₂, CHCl₃ and CH₃OH, (iv) CuCl₂, DBU, 1-octanol for **3a**, **3c**, **3d** and **3e**; CuCl₂, DBU and 1-hexanol for **3b**, **3f** and **3g**. DMF = *N,N'*-dimethylformamide, DMA = *N,N'*-dimethylacetamide and DBU = 1,8-diazabicyclo[5.4.0]-undec-7-ene.

3-Methoxyphenol (4c). A mixture of resorcinol (2.67 g, 24.3 mmol), K₂CO₃ (5.30 g, 38.3 mmol) and dry DMF (30 ml) placed in a 100 ml three-necked flask was stirred at 110 °C under a nitrogen atmosphere for 20 min. Then, iodomethane (7.86 g, 55.4 mmol) was added to the mixture and it was stirred at 110 °C under a nitrogen atmosphere for 1 h. After cooling to rt, the reaction mixture was extracted with chloroform and washed with water. The organic layer was dried over Na₂SO₄ overnight. After removing the Na₂SO₄ by filtration, the filtrate was evaporated *in vacuo* using an evaporator. The residue was purified by column chromatography (silica gel, chloroform, *R_f* = 0.18) to obtain 0.882 g of reddish brown liquid. Yield = 29.4%.

¹H-NMR (CDCl₃; TMS) δ = 7.13 (t; *J* = 9.60 Hz; 1H, Ar-H), 6.49 (d; *J* = 9.9 Hz; 1H, Ar-H), 6.45–6.39 (m; 2H, Ar-H), 5.67 (s; 1H, –OH), 3.77 (s; 1H, –OCH₃). IR (KBr, cm^{–1}); 3363 (–OH), 2968 (–CH₃), 2842 (–OCH₃).

4,5-Bis(3-methoxyphenoxy)phthalonitrile (5c). In a 100 ml three-necked flask, a mixture of 3-methoxyphenol (**4c**) (0.780 g, 6.28 mmol), K₂CO₃ (6.37 g, 46.1 mmol) and dry DMA (30 ml) was stirred at 110 °C under a nitrogen atmosphere for 15 min. Then, 4,5-dichlorophthalonitrile (0.566 g, 2.87 mmol) was added to the mixture and it was stirred at 110 °C under a nitrogen atmosphere for 3 h. After cooling to rt, the reaction mixture was extracted with diethyl ether and washed with water. The organic layer was dried over Na₂SO₄ overnight. After removing Na₂SO₄ by filtration, the filtrate was evaporated *in vacuo* using an

evaporator. The residue was purified by column chromatography (silica gel, dichloromethane, *R_f* = 0.53) to obtain 0.856 g of white solid. Yield = 80.8%. M.p. = 134 °C.

¹H NMR (CDCl₃; TMS) δ = 7.35 (t; *J* = 8.08 Hz; 2H, CN-Ar-H), 7.20 (s; 2H, Ar-O-Ar-H), 6.83 (d; *J* = 8.84 Hz; 2H, Ar-O-Ar-H), 6.66–6.61 (m; 4H, Ar-O-Ar-H), 3.82 (s; 6H, –OCH₃). IR (KBr, cm^{–1}); 2920 (–CH₃), 2837 (–OCH₃), 2222 (–CN).

4,5-Diphenoxyphthalonitrile (5a). Yield = 78.9%. M.p. = 147.9 °C. ¹H-NMR (CDCl₃; TMS) δ = 7.78 (s; 2H, NC-Ar-H), 7.43 (t; *J* = 8.00 Hz; 4H, Ar-O-Ar-H), 7.23 (t; *J* = 8.00 Hz; 2H, Ar-O-Ar-H), 7.10 (d; *J* = 8.00 Hz; 4H, Ar-O-Ar-H). IR (KBr, cm^{–1}); 2249 (–CN).

4,5-Bis(2-methoxyphenoxy)phthalonitrile (5b). Yield = 92.8%. M.p. = 138.2 °C. ¹H NMR (CDCl₃; TMS) δ = 7.22 (dd; *J*₁ = 8.08 Hz, *J*₂ = 7.83 Hz; 2H, NC-Ar-H), 7.10 (d; *J* = 8.09 Hz; 2H, Ar-O-Ar-H), 6.98 (dd; *J*₁ = 8.84 Hz, *J*₂ = 8.08 Hz; 4H, Ar-O-Ar-H), 6.86 (s; 2H, Ar-O-Ar-H), 3.75 (s; 6H, –OCH₃). IR (KBr, cm^{–1}); 2930, 2820 (–CH₃), 2210 (–CN).

4,5-Bis(4-methoxyphenoxy)phthalonitrile (5d). Yield = 93.4%. M.p. = 158.0 °C. ¹H NMR (CDCl₃; TMS) δ = 6.98 (m; 6H, NC-Ar-H and Ar-O-Ar-H), 6.91 (d; *J* = 8.84 Hz; 4H, Ar-O-Ar-H), 3.79 (s; 6H, –OCH₃). IR (KBr, cm^{–1}); 2912 (–CH₃), 2233 (–CN).

4,5-Bis(3,4-dimethoxyphenoxy)phthalonitrile (5e). Yield = 13.3%. M.p. = 189 °C. ¹H NMR (CDCl₃; TMS) δ = 7.10 (s; 2H, NC-Ar-H), 6.92 (d; *J* = 8.84 Hz; 2H, Ar-O-Ar-H), 6.67 (d; *J* = 9.16 Hz, 4H, Ar-O-Ar-H), 3.93 (s; 6H, –OCH₃), 3.88 (s; 6H, –OCH₃). IR (KBr, cm^{–1}); 2930, 2836 (–CH₃), 2233 (–CN).

Table 1 Yields, MALDI-TOF mass spectral data and elemental analysis data of **3a–g**^a

Compound	Yield (%)	Mol. formula (exact mass)	Observed mass	Mol. formula (average mass)	Element analysis; found (%) (calculated (%))		
					C	H	N
3a : (PhO) ₈ PcCu	48.4	C ₈₀ H ₄₈ N ₈ O ₈ Cu(1311.29)	1311.17	C ₈₀ H ₄₈ N ₈ O ₈ Cu(1312.87)	—	—	—
3b : [(<i>o</i> -C ₁)PhO] ₈ PcCu	65.5	C ₈₈ H ₆₄ N ₈ O ₁₆ Cu(1551.38)	1551.27	C ₈₈ H ₆₄ N ₈ O ₁₆ Cu(1553.04)	68.06 (68.44)	4.49 (4.15)	6.92 (7.22)
3c : [(<i>m</i> -C ₁)PhO] ₈ PcCu	66.7	C ₈₈ H ₆₄ N ₈ O ₁₆ Cu(1551.38)	1551.24	C ₈₈ H ₆₄ N ₈ O ₁₆ Cu(1553.04)	67.76 (68.44)	4.14 (4.15)	7.12 (7.22)
3d : [(<i>p</i> -C ₁)PhO] ₈ PcCu	35.6	C ₈₈ H ₆₄ N ₈ O ₁₆ Cu(1551.38)	1551.29	C ₈₈ H ₆₄ N ₈ O ₁₆ Cu(1553.04)	—	—	—
3e : {[<i>m,p</i> -(C ₁) ₂]PhO} ₈ PcCu	39.0	C ₉₆ H ₈₀ N ₈ O ₂₄ Cu(1791.46)	1791.27	C ₉₆ H ₈₀ N ₈ O ₂₄ Cu(1793.29)	—	—	—
3f : {[<i>m,m'</i> -(C ₁) ₂]PhO} ₈ PcCu	53.0	C ₉₆ H ₈₀ N ₈ O ₂₄ Cu(1791.46)	1791.37	C ₉₆ H ₈₀ N ₈ O ₂₄ Cu(1793.29)	—	—	—
3g : {[<i>m,p,m'</i> -(C ₁) ₃]PhO} ₈ PcCu	80.5	C ₁₀₄ H ₉₆ N ₈ O ₃₂ Cu(2031.55)	2031.58	C ₁₀₄ H ₉₆ N ₈ O ₃₂ Cu(2033.46)	61.59 (61.43)	4.46 (4.76)	5.63 (5.51)

^a —: this compound did not completely burn out, so the observed carbon content was lower by several percent than the calculated values. Therefore, these elemental analysis data are omitted here.

4,5-Bis(3,5-dimethoxyphenoxy)phthalonitrile (5f). Yield = 21.2%. M.p. = 263.4 °C. ¹H NMR (CDCl₃; TMS) δ = 7.12 (s; 2H, NC-Ar-H), 6.30 (t, *J* = 2.78 Hz; 2H, Ar-O-Ar-H), 6.15 (s; 4H, Ar-O-Ar-H), 3.72 (s; 12H, -OCH₃). IR (KBr, cm⁻¹); 2923, 2853 (-CH₃), 2233 (-CN).

4,5-Bis(3,4,5-trimethoxyphenoxy)phthalonitrile (5g). Yield = 76.8%. M.p. = 230.2 °C. ¹H NMR (CDCl₃; TMS) δ = 7.42 (s; 2H, NC-Ar-H), 6.01–5.92 (m; 4H, Ar-O-Ar-H), 3.71 (s; 18H, -OCH₃). IR (KBr, cm⁻¹); 2943, 2833 (-CH₃), 2233 (-CN).

[(*m*-C₁)PhO]₈PcCu (3c). In a 50 ml three-necked flask, a mixture of 4,5-bis(3-methoxy-phenoxy)phthalonitrile (**5c**) (0.505 g, 1.35 mmol), 1-octanol (5 ml), CuCl₂ (0.103 g, 0.766 mmol) and DBU (4 drops) was refluxed under a nitrogen atmosphere for 17 h. After cooling to rt, the reaction mixture was poured into methanol to precipitate the target compound. The methanolic layer was removed by filtration and then the resulting precipitate was washed with methanol, ethanol and acetone, respectively. The residue was purified by column chromatography (silica gel, chloroform : THF = 9 : 1, *R*_f = 0.70) and recrystallized from ethyl acetate to obtain 0.347 g of green solid. Yield = 66.7%.

MALDI-TOF mass data for **3a–g**: see Table 1.

Elemental analysis data for **3b, c, g**: see Table 1.

UV-vis spectral data **3b, c, e–g**: see Table 2.

2.2 Measurements

The compounds synthesized here were identified with a ¹H-NMR spectrometer (BRUKER Ultrashield 400 MHz), a FT-IR

spectrometer (Nicolet NEXUS 670), an elemental analyzer (Perkin-Elmer elemental analyzer 2400) and a MALDI-TOF mass spectrometer (AutoflexIII-2S). The elemental analysis data and the MALDI-TOF mass spectral data of the phthalocyanine derivatives **3a–g** are summarized in Table 1. Each of the electronic absorption spectra of all the phthalocyanine derivatives was recorded using a HITACHI U-4100 spectrophotometer and the data are summarized in Table 2. The phase transition behaviour was observed with a polarizing optical microscope (Nikon ECLIPSE E600 POL) equipped with a Mettler FP82HT hot stage and a Mettler FP-90 central processor, and a Shimadzu DSC-50 differential scanning calorimeter. The decomposition temperatures were measured by a Rigaku Thermo plus TG 820 thermogravimetry analyser. The mesophases were identified using a small angle X-ray diffractometer (Bruker Mac SAXS System) equipped with a temperature-dependent sample holder to clamp a Mettler FP82HT hot stage (see Fig. S1 and S2 in ref. 20), which was operated with a measurable range from 3.0 Å to 100 Å and a temperature range from rt to 375 °C.²⁰

3 Results and discussion

3.1 Synthesis

Table 1 lists the yields, and the MALDI TOF mass spectral data and the elemental analysis data of **3a–g**. As can be seen from this table, each of the mass spectral data of **3a–g** is in good accordance with the calculated exact mass. On the other hand,

Table 2 Electronic absorption spectral data of **3a–g**^a

Compound	Concentration ^b (× 10 ⁻⁵ mol l ⁻¹)	λ _{max} (nm) (log ε)						
		Soret-band					Q-band	
3a : (PhO) ₈ PcCu	—	—	—	—	—	—	—	—
3b : [(<i>o</i> -C ₁)PhO] ₈ PcCu	1.03	278.2 (4.77)	292.9 (4.75)	341.7 (4.84)	ca. 400 (4.43)	613.9 (4.58)	651.4 (4.54)	682.8 (5.33)
3c : [(<i>m</i> -C ₁)PhO] ₈ PcCu	1.03	—	284.2 (4.94)	341.7 (5.00)	ca. 400 (4.55)	614.6 (4.78)	650.7 (4.79)	681.5 (5.41)
3d : [(<i>p</i> -C ₁)PhO] ₈ PcCu	—	—	—	—	—	—	—	—
3e : {[<i>m,p</i> -(C ₁) ₂]PhO} ₈ PcCu	0.948	—	291.2 (4.86)	340.9 (4.88)	ca. 420 (4.29)	614.6 (4.60)	652.6 (4.59)	684.3 (5.31)
3f : {[<i>m,m'</i> -(C ₁) ₂]PhO} ₈ PcCu	1.00	—	289.2 (4.55)	342.2 (4.62)	ca. 390 (4.27)	614.5 (4.34)	651.1 (4.34)	682.4 (4.92)
3g : {[<i>m,p,m'</i> -(C ₁) ₃]PhO} ₈ PcCu	9.84	—	291.6 (3.85)	340 (3.97)	ca. 400 (4.46)	615.3 (3.71)	652.8 (4.69)	683.5 (5.45)

^a —: this derivative was insoluble in all the solvents. ^b In chloroform.

the elemental analysis data of **3b** and **3g** gave satisfactory values of C, H and N within $\pm 0.4\%$ deviation, but the observed value of C for **3c** is smaller by 0.68% than the calculated value and those of H and N are within $\pm 0.4\%$. Since each of the other derivatives of **3a**, **3d**, **3e** and **3f** was much less flammable than **3c**, which gave a much smaller carbon value by several per cent than the calculated value, these data are omitted in this table. This is characteristic of less flammable phthalocyanine derivatives.²¹ Table 2 summarizes the electronic absorption spectral data of **3a–g**. As can be seen from this table, each of the derivatives of **3b**, **3c** and **3e–g** gave a Q-band and Soret band characteristic to the PcCu complex with a D_{4h} symmetry. Since the derivatives, **3a** and **3d**, were insoluble in any solvents, no data are listed in this table. However, it could be confirmed from their MALDI-TOF mass spectra in Table 1 that the target derivatives, **3a** and **3d**, were surely synthesized. Also, it could be judged from both the MALDI-TOF mass spectra and the electronic absorption spectra of **3e** and **3f** in Tables 1 and 2 that they were surely prepared.

3.2 Phase transition behaviour

The phase transition behaviours of the phthalocyanine derivatives **3a–g** synthesized here are summarized in Table 3. These phase transitions were established by using a polarizing optical microscope (POM), a differential scanning calorimeter (DSC), a thermal gravity analyser (TGA) and a temperature-dependent small angle X-ray diffractometer. The phase transition behaviour of all the phthalocyanine derivatives **3a–g** is described in the following paragraphs.

As can be seen from Table 3, the $(\text{PhO})_8\text{PcCu}$ (**3a**) derivative with no methoxy group showed no mesophase, and only a crystalline (K) phase from rt to the decomposition temperature at 541 °C.

As can be seen from Table 3, the $[(o\text{-C}_1)\text{PhO}]_8\text{PcCu}$ (**3b**) derivative substituted by a methoxy group at an *ortho*-position in the phenoxy group showed a glassy $\text{Col}_{\text{ro}}(P2m)$ mesophase from rt for the freshly prepared virgin sample. When it was heated over the glass transition temperature at 87.4 °C, it relaxed to transform into crystalline phase K_1 ; on further heating, it transformed into another crystalline phase K_2 , which decomposed without weight loss (1st decomposition (decomp.)) just after melting at 299.4 °C, and then decomposed with some weight loss (2nd decomp.) at 402 °C. The two-step decomposition has already been seen in other liquid crystals based on phthalocyanine derivatives and has been studied in detail.²² In this paper, in the 1st decomp., the absorption spectra indicates that two neighbouring phenyl groups may form a ring by an intramolecular ring-closing reaction with losing two hydrogen atoms, which is, therefore, accompanied by almost no weight loss. The 2nd decomp. is a normal thermal decomposition accompanied by a large weight loss.

Fig. 2 shows a DSC thermogram on the first heating run of $[(o\text{-C}_1)\text{PhO}]_8\text{PcCu}$ (**3b**) together with a free energy *versus* temperature (G – T) diagram. As can be seen from this DSC thermogram, over the glass transition temperature (T_g) at 87.4 °C, there is an exothermic peak at 111.8 °C, which corresponds to the relaxation from the supercooled $\text{Col}_{\text{ro}}(P2m)$ mesophase to the crystalline phase K_1 ;²³ on further heating,

Table 3 Phase transition temperatures and enthalpy changes of **3a–g**^a

Compounds	Phase	T (°C) [ΔH (kJ mol ^{−1})]	Phase	relaxation
3a : $(\text{PhO})_8\text{PcCu}$	K	541	dc.	
3b : $[(o\text{-C}_1)\text{PhO}]_8\text{PcCu}$	Glassy $\text{Col}_{\text{ro}}(P2m)$	$T_g = 87.4$	K_1	
	K_1	177.3 [7.20]	K_2	
	K_2	299.4 [19.0]	I.L. (1st dc.)	
	I.L. (1st dc.)	402	2nd dc.	
3c : $[(m\text{-C}_1)\text{PhO}]_8\text{PcCu}$	Glassy $\text{Col}_{\text{ro}}(P2_1/a)$	$T_g = 69.9$	K	
	K	191.3 [13.4]	$\text{Col}_{\text{ro}1}(P2_1/a)$	
	$\text{Col}_{\text{ro}1}(P2_1/a)$	255.1 [2.69]	$\text{Col}_{\text{ro}2}(P2_1/a)$	
	$\text{Col}_{\text{ro}2}(P2_1/a)$	360.1 [10.7]	M_x (1st dc.)	
	M_x (1st dc.)	405	2nd dc.	
3d : $[(p\text{-C}_1)\text{PhO}]_8\text{PcCu}$	K	363	dc.	
3e : $[(m,p\text{-C}_1)_2]\text{PhO}]_8\text{PcCu}$	K	189.0 [21.5]	$\text{Col}_{\text{ro}}(P2_1/a)$	
	$\text{Col}_{\text{ro}}(P2_1/a)$	351.4 [41.8]	I.L. (1st dc.)	
	I.L. (1st dc.)	394	2nd dc.	
3f : $[(m,m'\text{-C}_1)_2]\text{PhO}]_8\text{PcCu}$	K	310.5 [14.6]	$\text{Col}_{\text{ro}}(C2/m)$ (1st dc.)	
	$\text{Col}_{\text{ro}}(C2/m)$ (1st dc.)	430	2nd dc.	
3g : $[(m,p,m'\text{-C}_1)_3]\text{PhO}]_8\text{PcCu}$	Glassy $\text{Col}_{\text{tet.o}}$	$T_g = 67.9$	K_1	
	K_1	157.5 [1.56]	K_2	
	K_2	262.1 [17.1]	$\text{Col}_{\text{tet.o}}$ (1st dc.)	
	$\text{Col}_{\text{tet.o}}$ (1st dc.)	346	2nd dc.	

^a Phase nomenclature: K = crystal, Col_{ro} = rectangular ordered columnar mesophase, M_x = unidentified mesophase, $\text{Col}_{\text{tet.o}}$ = tetragonal ordered columnar mesophase, I.L. = isotropic liquid and dc. = decomposition.

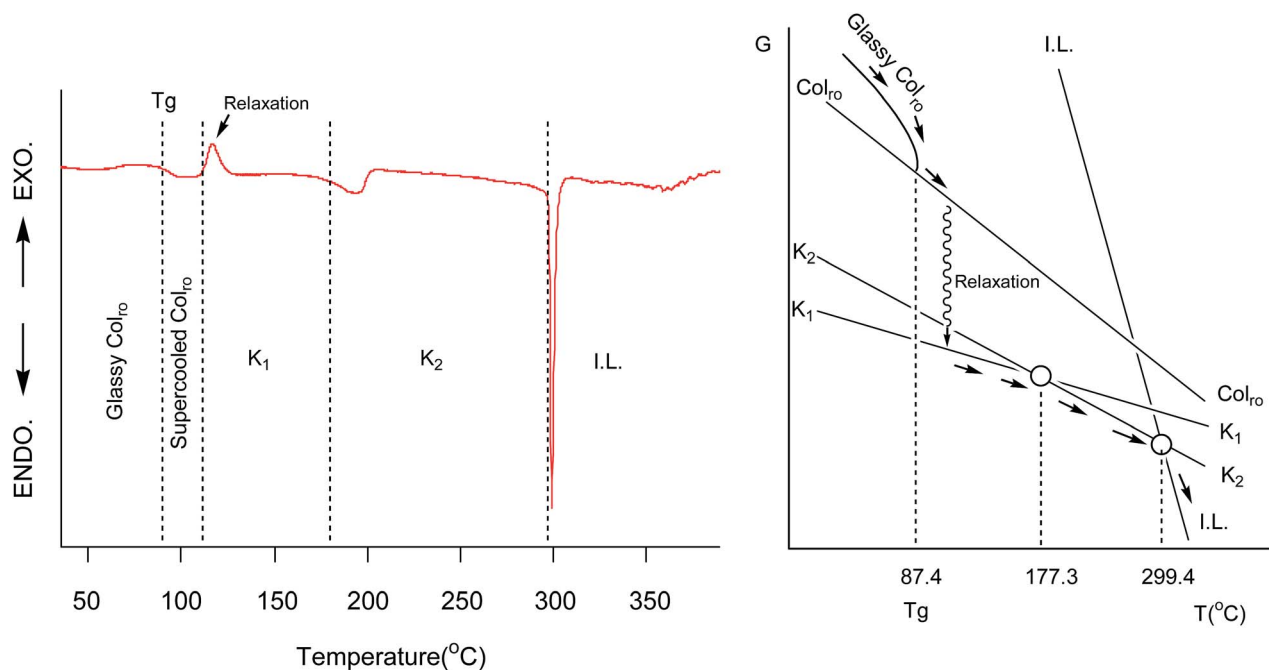


Fig. 2 DSC thermogram and G - T diagram of $[(o-C_1)PhO]_8PcCu$ (**3b**) on the 1st heating run.

there is a relatively broad endothermic peak at 177.3 °C, which is assigned to the solid–solid (K_1 – K_2) phase transition. On heating, there is a big sharp endothermic peak at 229.4 °C, which is assigned as the melting point, as under the microscope, we could observe that the crystals melted into an isotropic liquid (I.L.) at this temperature. Such monotropic glassy mesophase transformation behaviour can be rationally explained by using the G - T diagram, as illustrated in the right-hand side of Fig. 2. When the freshly prepared virgin sample was pressed between two glass plates, it was rigid. However, it is crystallographically mesomorphic from the X-ray structural analysis, as it does not have a 3D lattice, but instead a 2D rectangular lattice with a $P2m$ symmetry. Over T_g , this changes into the supercooled Col_{ro} mesophase, in which the more mobile molecules easily rearrange into the more stable crystalline phase K_1 by relaxation. This gives an exothermic peak. On heating, the K_1 phase transforms into another crystalline phase K_2 by a solid–solid phase transition at 177.3 °C. The crystalline phase K_2 transforms into I.L. at 229.4 °C. These phase transformations occur in the order of the arrows indicated in this G - T diagram, and furthermore, they can be rationally explained from a thermodynamic viewpoint.

As can be seen from Table 3, the $[(m-C_1)PhO]_8PcCu$ (**3c**) derivative substituted by a methoxy group at a *meta*-position in the phenoxy group also showed a glassy rectangular ordered columnar mesophase $Col_{ro}(P2_1/a)$ at rt for the freshly prepared virgin sample. When it was heated over the glass transition temperature at 69.9 °C, it relaxed into the crystalline phase K. On heating, this crystalline phase K transformed into the $Col_{ro1}(P2_1/a)$ mesophase and then another rectangular ordered columnar mesophase, $Col_{ro2}(P2_1/a)$. On further heating, it transformed into an unidentified mesophase M_x at 360.1 °C,

which decomposed without weight loss (1st decomp.) just after the transition, and then decomposed with weight loss (2nd decomp.) at 405 °C.

The $[(p-C_1)PhO]_8PcCu$ (**3d**) derivative substituted by a methoxy group at a *para*-position in the phenoxy group showed no mesophase, and only a crystalline phase (K) from rt to the decomposition temperature at 363 °C.

The $\{[m,m'-(C_1)_2]PhO\}_8PcCu$ (**3f**) derivative substituted by two methoxy groups at the *meta*- and *meta'*-positions in the phenoxy group showed a crystalline phase K from rt, which then melted into a $Col_{ro}(C2/m)$ mesophase at 310.5 °C. This gradually decomposed without weight loss (1st decomp.) over the melting point (mp), and then decomposed with weight loss (2nd decomp.) at 430 °C.

The $\{[m,p,m'-(C_1)_3]PhO\}_8PcCu$ (**3g**) derivative substituted by three methoxy groups at the *meta*-, *para*- and *meta'*-positions in the phenoxy group showed a glassy tetragonal ordered columnar ($Col_{tet,o}$) mesophase at rt. When it was heated over the glass transition temperature (T_g) at 67.9 °C, it relaxed into a crystalline phase K_1 . On further heating, the K_1 phase transformed into another crystalline phase K_2 at 157.5 °C. The K_2 phase melted into the $Col_{tet,o}$ mesophase at 262.1 °C. Over the mp, it gradually decomposed without weight loss (1st decomp.), and decomposed with weight loss (2nd decomp.) at 346 °C.

In our previous work on the long chain-substituted homologues of $(p-C_nOPhO)_8PcCu$, $(m-C_nOPhO)_8PcCu$ and $(o-C_nOPhO)_8PcCu$, we reported that the steric hindrance of a peripheral chain depends on its substitution position, and becomes bigger in the order of *para* position \rightarrow *meta* position \rightarrow *ortho* position, and that a greater steric hindrance induces a weaker interaction among the central Pc cores.²⁴ We compared the four present homologous PcCu derivatives **3a–d** with each

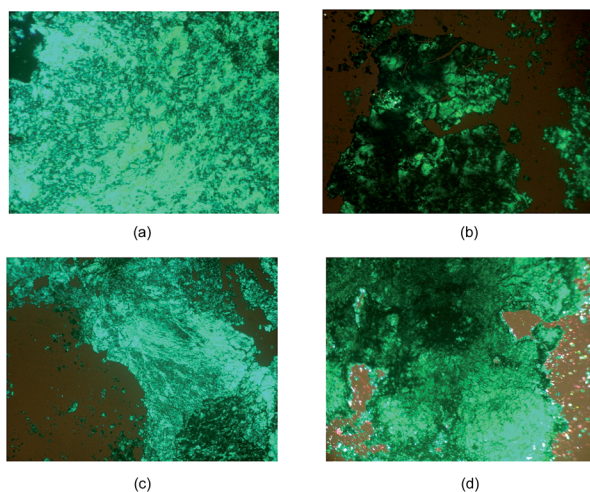


Fig. 3 Photomicrographs of (a) Col_{ro1}(P2₁/a) mesophase of [(*m*-C₁)PhO]₈PcCu (**3c**) at 230 °C, (b) Col_{ro}(P2₁/a) mesophase of {[*m,p*-(C₁)₂]PhO}₈PcCu (**3e**) at 250 °C, (c) Col_{ro}(P2₁/a) mesophase of {[*m,m'*-(C₁)₂]PhO}₈PcCu (**3f**) at 320 °C, and (d) Col_{tet,o} mesophase of {[*m,p,m'*-(C₁)₃]PhO}₈PcCu (**3g**) at 268 °C.

other, where the non-substituted derivative **3a** and the *para*-methoxy-substituted derivative **3d** show only a crystalline phase, the *meta*-methoxy-substituted derivative **3c** only shows enantiotropic mesophases, and the *ortho*-methoxy-substituted derivative **3b** only shows an isotropic liquid. The PhO group cannot freely rotate due to the neighbouring PhO group, so that the Ph plane twists *c.* 90° against that of the Pc core. Hence, the angle between the methoxy group and the Pc core become smaller in the order of *para* position → *meta* position → *ortho* position. The methoxy group at the *meta* position and *ortho* position on the Pc core plane become a steric hindrance to weaken the aggregation (=stacking) of the Pc cores. Additionally, the methoxy group at the *ortho* position covers the Pc core plane.

Therefore, the *meta*-methoxy-substituted derivative **3c** only shows enantiotropic mesophases, and the *ortho*-methoxy-substituted derivative **3b** only shows an isotropic liquid.

3.3 Polarizing optical microscopic observations

Fig. 3 shows the photomicrographs of the Pc derivatives, **3c**, **3e**, **3f** and **3g**, exhibiting mesophases. Fig. 3(a)–(d) are the

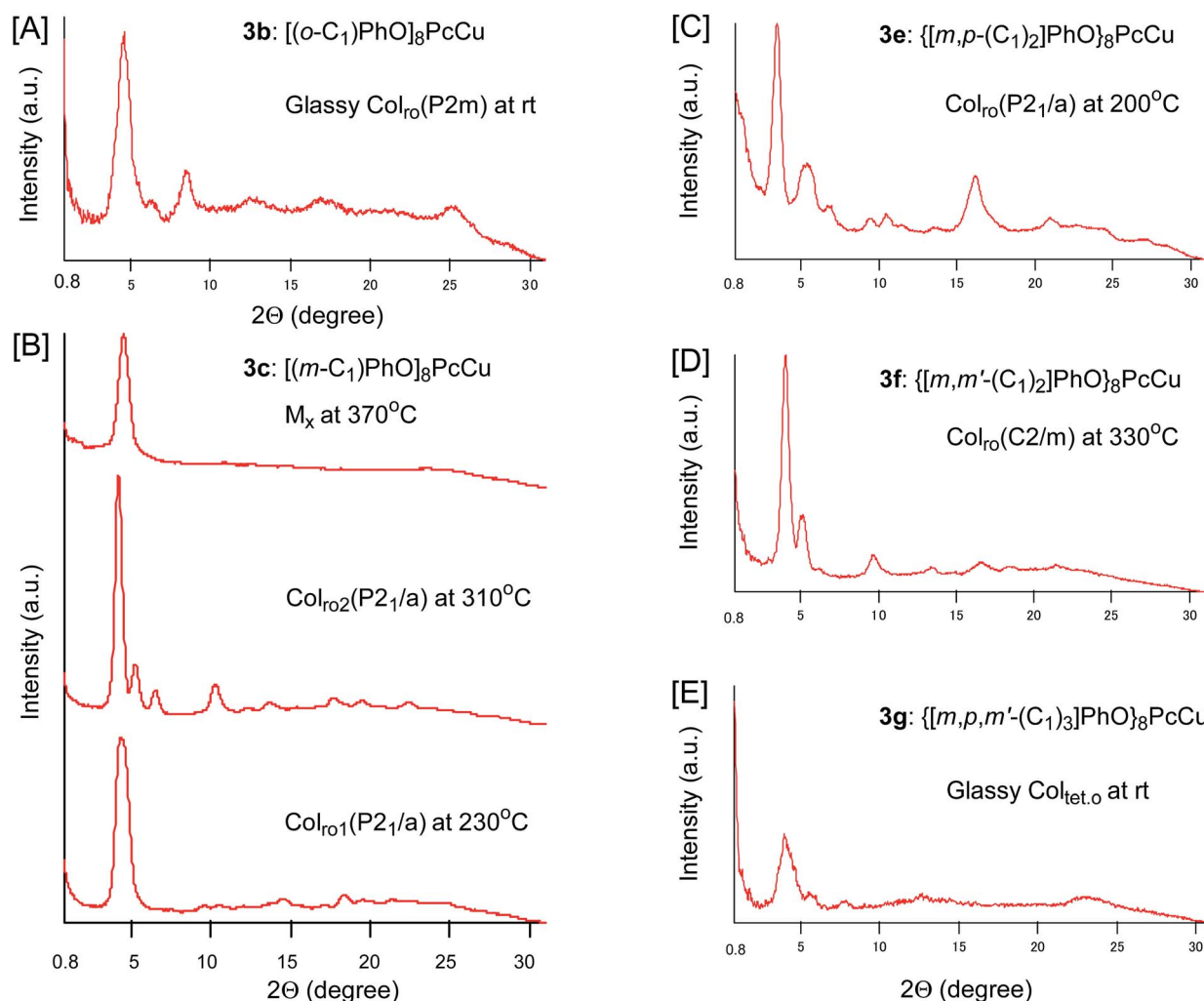


Fig. 4 XRD patterns of the mesophases: [A] [(*o*-C₁)PhO]₈PcCu (**3b**) at rt; [B] [(*m*-C₁)PhO]₈PcCu (**3c**) at 230 °C, 310 °C and 370 °C; [C] {[*m,p*-(C₁)₂]PhO}₈PcCu (**3e**) at 200 °C; [D] {[*m,m'*-(C₁)₂]PhO}₈PcCu (**3f**) at 330 °C; [E] {[*m,p,m'*-(C₁)₃]PhO}₈PcCu (**3g**) at rt.

Table 4 X-ray data of **3b**, **3c**, **3e**, **3f** and **3g**^a

Compound (mesophase)	Mesophase lattice constants (Å)	Peak no.	Spacing (Å)		Miller indices (<i>h k l</i>)
			Obs.	Calc.	
3b : [(<i>o</i> -C ₁)PhO] ₈ PcCu (glassy Col _{ro} (<i>P2m</i>) at rt)	<i>a</i> = 20.7 <i>b</i> = 19.2 <i>h</i> = 7.00 <i>Z</i> = 1.1 for ρ = 1.0	1	19.3	19.2	(010)
		2	13.9	14.1	(110)
		3	10.4	10.4	(200)
		4	7.00	—	<i>h</i>
		5	5.15	5.18	(400)
		6	3.53	3.52	(440)
3c : [(<i>m</i> -C ₁)PhO] ₈ PcCu (Col _{ro1} (<i>P2₁/a</i>) at 230 °C)	<i>a</i> = 29.4 <i>b</i> = 26.5 <i>h</i> = 6.09 <i>Z</i> = 2.0 for ρ = 1.1	1	20.1	19.7	(110)
		2	13.2	13.3	(020)
		3	11.8	12.1	(120)
		4	9.24	9.19	(310)
		5	8.46	8.46	(130)
		6	7.39	7.35	(400)
		7	6.51	6.47	(140)
		8	6.09	—	<i>h</i>
		9	5.17	5.22	(150)
		10	4.84	4.82	(610)
		11	4.54	4.60	(620)
		12	4.41	4.41	(060)
		13	4.15	4.15	(710)
(Col _{ro2} (<i>P2₁/a</i>) at 310 °C)	<i>a</i> = 33.6 <i>b</i> = 27.1 <i>h</i> = 5.00 <i>Z</i> = 2.0 for ρ = 1.1	1	21.1	21.1	(110)
		2	16.8	16.8	(200)
		3	13.6	13.6	(020)
		4	8.61	8.64	(320)
		5	7.18	7.14	(420)
		6	6.48	6.52	(510)
		7	5.73	5.80	(340)
		8	5.33	5.36	(150)
		9	5.00	—	<i>h</i>
		10	4.57	4.56	(450)
		11	4.32	4.32	(640)
		12	3.97	3.98	(460)
		13	3.72	3.74	(560)
		14	3.55	3.55	(840)
		15	3.42	3.42	(080)
(M _x at 370 °C)		1	19.5	—	—
		2	ca. 3.8	—	<i>h</i>
3e : {[<i>m</i> , <i>p</i> -(C ₁) ₂]PhO} ₈ PcCu (Col _{ro} (<i>P2₁/a</i>) at 200 °C)	<i>a</i> = 40.2 <i>b</i> = 33.1 <i>h</i> = 4.21 <i>Z</i> = 1.9 for ρ = 1.0	1	25.5	25.5	(110)
		2	16.5	16.5	(020)
		3	12.9	12.8	(220)
		4	9.38	9.60	(410)
		5	8.41	8.51	(330)
		6	6.50	6.49	(530)
		7	5.50	5.51	(060)
		8	4.21	—	<i>h</i>
3f : {[<i>m</i> , <i>m'</i> -(C ₁) ₂]PhO} ₈ PcCu (Col _{ro} (<i>C2/m</i>) at 330 °C)	<i>a</i> = 34.2 <i>b</i> = 28.6 <i>h</i> = 4.80 <i>Z</i> = 1.9 for ρ = 1.2	1	21.8	21.9	(110)
		2	17.3	17.1	(200)
		3	14.3	14.3	(020)
		4	9.18	9.18	(130)
		5	6.56	6.59	(240)
		6	5.34	5.30	(620)
		7	4.80	—	<i>h</i>
		8	4.15	4.16	(460)

Table 4 (Contd.)

Compound (mesophase)	Mesophase lattice constants (Å)	Peak no.	Spacing (Å)		Miller indices (<i>h k l</i>)
			Obs.	Calc.	
3g : $\{[m,p,m'-(C_1)_3]PhO\}_8PcCu$ (glassy Col _{tet,o} at rt)	$a = 22.3$ $h = 3.87$ $Z = 1.0$ for $\rho = 1.0$	1	22.3	22.3	(100)
		2	15.9	15.8	(110)
		3	11.4	11.2	(200)
		4	7.00	7.07	(310)
		5	3.87	—	h

^a h : stacking distance = (0 0 1), ρ : assumed density (g cm⁻³).

photomicrographs of $[(m-C_1)PhO]_8PcCu$ (**3c**) at 230 °C, $\{[m,p-(C_1)_2]PhO\}_8PcCu$ (**3e**) at 250 °C, $\{[m,m'-(C_1)_2]PhO\}_8PcCu$ (**3f**) at 320 °C, and $\{[m,p,m'-(C_1)_3]PhO\}_8PcCu$ (**3g**) at 268 °C, respectively. Each of these *Pc* derivatives decomposes without showing an isotropic liquid and/or rapidly decomposes just after melting into isotropic liquid, so that they do not show a natural texture which would be obtained by slow cooling from an isotropic liquid. However, as can be seen from the photomicrographs in Fig. 3, each of the derivatives was spread out and showed stickiness together with birefringence when the cover glass plate was pressed at the temperature denoted below the photomicrograph. Hence, these states could be identified as mesophases.

3.4 Temperature-dependent X-ray diffraction measurements

In order to clarify the precise mesophase structure, temperature-dependent small angle X-ray diffraction measurements were carried out for the *Pc* derivatives, **3b**, **3c**, **3e**, **3f** and **3g**, showing mesomorphism. These X-ray diffraction (XRD) patterns and their X-ray data are summarized in Fig. 4 and Table 4, respectively. As can be seen from the XRD patterns, no broad halo around $2\theta = 20^\circ$ due to the molten long alkyl chains are observed, although the halo can be generally observed for conventional liquid crystals. This is a result of there being no long alkyl chains in the present liquid crystals with only the shortest methoxy groups.

[(p-C₁)PhO]₈PcCu (3b). The $[(p-C_1)PhO]_8PcCu$ (**3b**) derivative substituted by a methoxy group at the *para* position of the phenoxy group shows a glassy mesophase at rt. As can be seen from the XRD pattern in Fig. 4[A] and the X-ray data in Table 4, this glassy mesophase gave six reflection peaks. All the peaks except for Peak no. 4 could be well assigned to the reflections from a 2D rectangular lattice with a *P2m* symmetry and the lattice constants, $a = 20.7$ Å and $b = 19.2$ Å, could be determined from the Reciprocal Lattice Calculation Method.²⁵ Peak no. 4 could be assigned to the stacking distance ($h = 7$ Å) among the central *PcCu* cores. Although the stacking distance of 7 Å is very long in comparison with the stacking distances usually observed at 4–5 Å for conventional rectangular columnar mesophases, this stacking distance can be proven as a proper value from the *Z* value calculation.²⁵

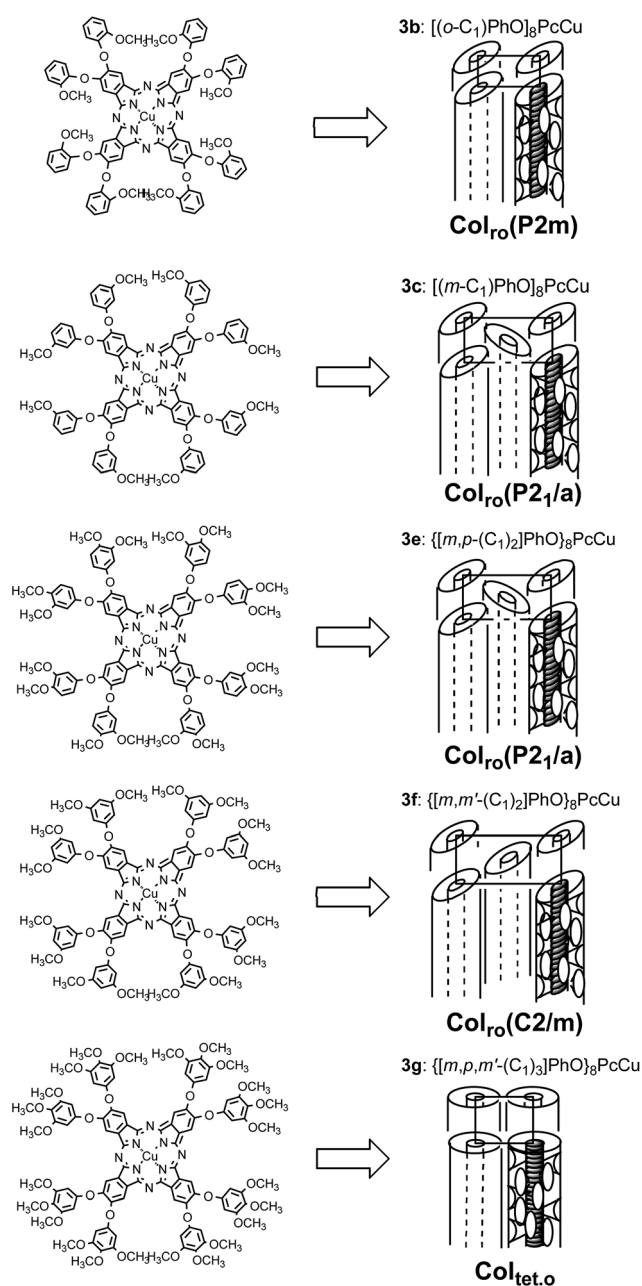


Fig. 5 Dependence of the mesophase structure on the bulky substituent for flying-seed-like liquid crystals based on PhO_8PcCu .

The number (Z) of molecules in a lattice can be calculated from this stacking distance ($h = 7 \text{ \AA}$) and the lattice constant of the 2D rectangular lattice ($a = 20.7 \text{ \AA}$ and $b = 19.2 \text{ \AA}$) listed in Table 4. Where ρ , V , N and M are the density of the mesophase, the volume of the unit lattice, Avogadro's number and the molecular weight, respectively, the Z value can be obtained from the following equation:

$$Z = (\rho VN)/M = \{\rho [a \times b \times h]N\}/M = [1.0 (\text{g cm}^{-3}) \times (20.7 \times 10^{-8} \text{ cm}) \times (19.2 \times 10^{-8} \text{ cm}) \times (7.00 \times 10^{-8} \text{ cm}) \times 6.02 \times 10^{23} (\text{mol}^{-1})]/1553.04 (\text{g mol}^{-1}) = 1.08 \approx 1$$

The calculated value $Z \approx 1$ is the same as the theoretical number of molecules in a 2D rectangular lattice with a $P2m$ symmetry: $Z = 1.0$. Therefore, this big stacking distance $h = 7 \text{ \AA}$ is a rationally proper value.

When this glassy $\text{Col}_{\text{ro}}(P2m)$ mesophase was heated over the glass transition temperature at $87.4 \text{ }^\circ\text{C}$, it relaxed into a crystalline phase K_1 . The XRD pattern of the K_1 phase gave a lot of sharp peaks in all the regions, from low angles to high angles. This apparently implies that the glassy mesophase is crystallized. On heating to the melting point from $299.4 \text{ }^\circ\text{C}$, no XRD pattern of the $\text{Col}_{\text{ro}}(P2m)$ appeared again. Therefore, the $\text{Col}_{\text{ro}}(P2m)$ mesophase is considered monotropic and appears only for the freshly prepared virgin sample as a glassy $\text{Col}_{\text{ro}}(P2m)$ mesophase.

$[(m\text{-}C_1)\text{PhO}]_8\text{PcCu}$ (3c). Fig. 4[B] shows the XRD patterns of the $[(m\text{-}C_1)\text{PhO}]_8\text{PcCu}$ (3c) derivatives at $230 \text{ }^\circ\text{C}$, $310 \text{ }^\circ\text{C}$ and $370 \text{ }^\circ\text{C}$. As can be seen from the XRD patterns in Fig. 4[B] and the X-ray data in Table 4, the XRD pattern at $230 \text{ }^\circ\text{C}$ gave thirteen peaks. All the peaks except for Peak no. 8 could be well assigned to the reflections from a 2D rectangular lattice with a $P2_1/a$ symmetry and the lattice constants, $a = 29.4 \text{ \AA}$ and $b = 26.5 \text{ \AA}$. Peak no. 8 could be assigned to the stacking distance ($h = 6.09 \text{ \AA}$).

Hence, this mesophase could be identified as a $\text{Col}_{\text{ro}}(P2_1/a)$ mesophase. The XRD pattern at $310 \text{ }^\circ\text{C}$ gave fifteen peaks. In the same manner as described above, this mesophase could also be identified as another $\text{Col}_{\text{ro}}(P2_1/a)$ mesophase with different lattice constants and stacking distance: $a = 33.6 \text{ \AA}$ and $b = 27.1 \text{ \AA}$, $h = 5 \text{ \AA}$. Thus, this derivative exhibited two $\text{Col}_{\text{ro}}(P2_1/a)$ mesophases with different sets of lattice constants and stacking distances. On further heating, it showed an unidentified mesophase M_x . As can be seen from the XRD pattern in Fig. 4[B] and the X-ray data in Table 4, the M_x mesophase gave only two peaks, so that we could not identify it.

$\{[m,p\text{-}(C_1)_2]\text{PhO}\}_8\text{PcCu}$ (3e). In the same manner described above, the mesophase at $200 \text{ }^\circ\text{C}$ could be identified as a $\text{Col}_{\text{ro}}(P2_1/a)$ mesophase having lattice constants: $a = 40.2 \text{ \AA}$, $b = 33.1 \text{ \AA}$ and $h = 4.21 \text{ \AA}$.

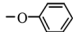
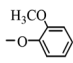
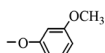
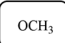
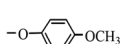
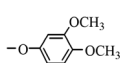
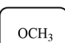
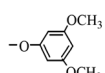
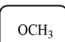
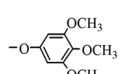
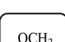
$\{[m,m'\text{-}(C_1)_2]\text{PhO}\}_8\text{PcCu}$ (3f). In the same manner as described above, the mesophase at $330 \text{ }^\circ\text{C}$ could be identified as a $\text{Col}_{\text{ro}}(C2/m)$ mesophase with a different symmetry $C2/m$ with lattice constants: $a = 34.2 \text{ \AA}$ and $b = 28.6 \text{ \AA}$, and $h = 4.80 \text{ \AA}$.

$\{[m,p,m'\text{-}(C_1)_3]\text{PhO}\}_8\text{PcCu}$ (3g). The mesophase in this derivative 3g decomposed so rapidly in the mesomorphic temperature region that the XRD pattern was measured for the glassy mesophase at rt. As can be seen from Fig. 4[E] and Table 4, this glassy mesophase gave five reflections. All the peaks except for Peak no. 5 could be assigned to the reflections from a 2D tetragonal lattice with the lattice constant, $a = 22.3 \text{ \AA}$. Peak no. 5 could be assigned to the stacking distance ($h = 3.87 \text{ \AA}$).

3.5 Mesomorphism depending on the number and position of the methoxy group

Fig. 5 illustrates the dependence of the mesophase structure on the bulky substituent for the present flying-seed-like liquid crystals based on $(\text{PhO})_8\text{PcCu}$. As can be seen from this figure, the bulkier the substituent becomes, the higher the symmetry of

Table 5 Appearance of mesomorphism for the flying-seed-like compounds (3a–g) based on $(\text{PhO})_8\text{PcCu}^a$

Compound	Substituent	X_0	X_m	X_p	$X_{m'}$	Appearance of mesophase
3a: $(\text{PhO})_8\text{PcCu}$		H	H	H	H	×
3b: $[(o\text{-}C_1)\text{PhO}]_8\text{PcCu}$		OCH_3	H	H	H	\triangle (Monotropic)
3c: $[(m\text{-}C_1)\text{PhO}]_8\text{PcCu}$		H		H	H	\bigcirc
3d: $[(p\text{-}C_1)\text{PhO}]_8\text{PcCu}$		H	H	OCH_3	H	×
3e: $\{[m,p\text{-}(C_1)_2]\text{PhO}\}_8\text{PcCu}$		OCH_3		H	H	\bigcirc
3f: $\{[m,m'\text{-}(C_1)_2]\text{PhO}\}_8\text{PcCu}$		H		H	OCH_3	\bigcirc
3g: $\{[m,p,m'\text{-}(C_1)_3]\text{PhO}\}_8\text{PcCu}$		H		OCH_3	OCH_3	\bigcirc

^a ×: no mesophase appears; \triangle : monotropic mesophase appears; \bigcirc : enantiotropic mesophase appears.

the mesophase becomes, in the order of **c**, **e** → **f** → **g**. Since the bulkiness of the substituent of **c** and **e** induced by the flip-flop is the same, it may result in the same symmetry of $P2_1/a$ for **3c** and **3e**.

Table 5 summarizes the appearance of the mesomorphism of the present $(\text{PhO})_8\text{PcCu}$ derivatives **3a–g**. As can be seen from this table, the derivatives with methoxy group(s) at the *meta* position(s), **3c**, **3e**, **3f** and **3g**, show enantiotropic mesophase(s), whereas neither the derivative with no methoxy group, **3a**, nor the derivative with a methoxy group at the *para* position, **3d**, show a mesophase. The derivative with a methoxy group at the

ortho position, **3b**, shows a monotropic mesophase. The reason for this could be due to the excluded volume of the phenoxy group originated by flip-flop and steric hindrance of the methoxy group(s) for stacking of the *Pc* cores.

Fig. 6 illustrates three representative molecular structures of $(\text{PhO})_8\text{PcCu}$ (**3a**) showing no mesophase, $[(o\text{-C}_1)\text{PhO}]_8\text{PcCu}$ (**3b**) showing a monotropic mesophase, and $[(m\text{-C}_1)\text{PhO}]_8\text{PcCu}$ (**3c**) showing an enantiotropic mesophase. In this figure are also schematically illustrated the excluded volume from flip-flopping the substituent as a cone. As can be seen from this figure, the excluded volume in **3a** showing no mesophase is obviously smaller than the excluded volume in **3c** showing a mesophase. Hence, the excluded volume may be strongly related with the appearance of mesomorphism: it could be that the excluded volume originated by the flip-flopping of the substituent is too small to form the part soft enough for the appearance of a mesophase.

Accordingly, when a methoxy group is substituted at the *para* position in the phenoxy group, such as in **3d**, the excluded volume is too small to show a mesophase. When a methoxy group is substituted at an *ortho* position, such as in **3b**, the excluded volume is the same as that of **3c**. However, **3c** shows enantiotropic mesophases, whereas **3b** show a monotropic mesophase. This may be attributed to the steric hindrance of the *ortho*-methoxy group that covers the *Pc* core plane, as already mentioned in the previous Section 3.2. The steric hindrance may block the stacking of the central *Pc* cores and suppress the formation of the columnar mesophase. This may decrease the clearing point of the mesophase and relatively elevate the melting point of the crystalline phase to induce the monotropic mesophase for **3b**.

The driving force of columnar structure formation for disk-like molecules is intermolecular π - π interactions among the central cores. It has already reported that peripheral substituents have an effect on the columnar mesophase structures.^{26–28}

Since the intermolecular interaction among the central cores of a series of the present *PcCu*-based liquid crystals is also affected by the peripheral bulky substituents, **b**, **c**, **e**, **f** and **g**, the various kinds of columnar mesophases, $\text{Col}_{\text{ro}}(P2m)$, $\text{Col}_{\text{ro}}(P2_1/a)$, $\text{Col}_{\text{ro}}(C2/m)$ and $\text{Col}_{\text{tet},o}$, may be formed. It is very interesting that the appearance of mesomorphism and the mesophase structures are greatly affected by the number and position of the methoxy groups.

4 Conclusion

We have synthesized a novel series of flying-seed-like derivatives (**3a–g**) based on phthalocyaninato copper(II) (abbreviated as *PcCu*) substituted by bulky groups {*PhO* (**a**), (*o*-*C*₁)*PhO* (**b**), (*m*-*C*₁)*PhO* (**c**), (*p*-*C*₁)*PhO* (**d**), [*m,p*-(*C*₁)₂]*PhO* (**e**), [*m,m'*-(*C*₁)₂]*PhO* (**f**), [*m,p,m'*-(*C*₁)₃]*PhO* (**g**)} in order to investigate how they show mesomorphism depending on the number and position of methoxy groups. As a result, $(\text{PhO})_8\text{PcCu}$ (**3a**) and $[(p\text{-C}_1)\text{PhO}]_8\text{PcCu}$ (**3d**) were seen to show no mesophase, whereas $[(m\text{-C}_1)\text{PhO}]_8\text{PcCu}$ (**3c**), $\{[m,p\text{-}(C_1)_2]\text{PhO}\}_8\text{PcCu}$ (**3e**), $\{[m,m'\text{-}(C_1)_2]\text{PhO}\}_8\text{PcCu}$ (**3f**), and $\{[m,p,m'\text{-}(C_1)_3]\text{PhO}\}_8\text{PcCu}$ (**3g**) show various kinds of columnar mesophases of $\text{Col}_{\text{ro}}(P2_1/a)$, $\text{Col}_{\text{ro}}(P2_1/a)$, $\text{Col}_{\text{ro}}(C2/m)$

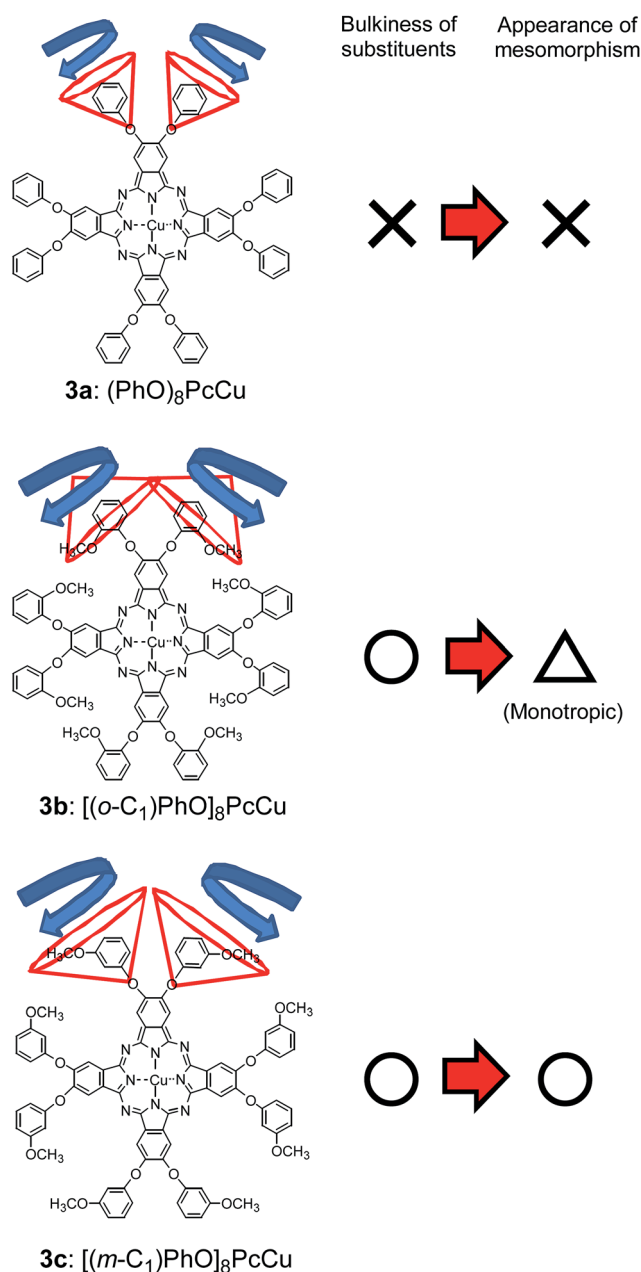


Fig. 6 Appearance of mesomorphism depending on bulkiness of the substituents. X: no mesophase appears; Δ : monotropic mesophase appears; \circ : enantiotropic mesophase appears.

and Col_{tet.o}, respectively; [(*o*-C₁)PhO]₈PcCu (**3b**) shows a monotropic Col_{ro}(*P2m*) mesophase. Thus, the derivative substituted by a methoxy group at a *para* position (**3d**) does not show mesomorphism because the excluded volume originated by the flip-flopping substituent is small. On the other hand, the derivatives substituted by (a) methoxy group(s) at (a) *meta* position(s) (**3c**, **e**, **f** and **g**) show enantiotropic mesomorphism because the excluded volume is big enough. The derivative substituted by a methoxy group at an *ortho* position (**3b**) shows monotropic mesomorphism, as the excluded volume is big enough but the steric hindrance may block the stacking of the central Pc cores.

In this work, we have revealed that mesomorphism could be induced by these novel bulky substituents instead of using long alkyl chains, and that the mesophase structures are greatly affected by the number and position of the methoxy groups. It is very interesting that the derivatives with methoxy group(s) at the *meta* position(s), *i.e.*, **3c**, **3e**, **3f** and **3g**, tend to show enantiotropic mesophase(s), whereas neither the derivative with no methoxy group, **3a**, nor the derivative with a methoxy group at the *para* position, **3d**, show a mesophase. We believe that the present examples of novel flying-seed-like liquid crystals will greatly contribute to exploring a new field of liquid crystal science.

References

- 1 Database of liquid crystalline compounds for personal computer, LiqCryst Version 5, ed. V. Vill, LCI Publisher and Fujitsu Kyushu Systems Limited, 2010.
- 2 Handbook of Liquid Crystals, ed. D. Demus, J. W. Goodby, G. W. Gray, H. W. Spiess and V. Vill, Wiley-VCH, 1998, vol. 4.
- 3 D. Vorländer, *Ber. Dtsch. Chem. Ges.*, 1911, **43**, 3120–3125.
- 4 D. Demus, H. Sackmann and K. Seibert, *Wiss. Z. – Martin-Luther-Univ. Halle-Wittenberg, Math.-Naturwiss. Reihe*, 1970, **19**, 47–62.
- 5 P. Ferloni, M. Sanesi, P. L. Tonelli and P. Franzosini, *Z. Naturforsch., A: Phys., Phys. Chem., Kosmophys.*, 1978, **33**, 240–242.
- 6 M. Sanesi, P. Ferloni, G. Spinolo and P. L. Tonelli, *Z. Naturforsch., A: Phys., Phys. Chem., Kosmophys.*, 1978, **33**, 386–388.
- 7 R. van Deun, J. Ramaekers, P. Nockemann, K. van Hecke, L. van Meervelt and K. Binnemans, *Eur. J. Inorg. Chem.*, 2005, 563–571.
- 8 K. Ohta, T. Shibuya and M. Ando, *J. Mater. Chem.*, 2006, **16**, 3635–3639.
- 9 N. Usol'tseva, V. Bykova, G. Ananjeva and N. Zharnikova, *Mol. Cryst. Liq. Cryst.*, 2014, **411**, 1371–1378.
- 10 N. Zharnikova, N. Usol'tseva, E. Kudrik and M. Theakkat, *J. Mater. Chem.*, 2009, **19**, 3161–3167.
- 11 Y. Takagi, K. Ohta, S. Shimosugi, T. Fujii and E. Itoh, *J. Mater. Chem.*, 2012, **22**, 14418–14425.
- 12 A. Hachisuga, M. Yoshioka, K. Ohta and T. Itaya, *J. Mater. Chem.*, 2013, **1**, 5315–5321.
- 13 C. Eaborn and N. H. Hartshorne, *J. Chem. Soc.*, 1955, 549–555.
- 14 J. D. Buning, J. E. Lydon, C. Eaborn, P. M. Jackson, J. W. Goodby and G. W. Gray, *J. Chem. Soc., Faraday Trans. 1*, 1982, **78**, 713–724.
- 15 S. Basurto, S. Garcia, A. G. Neo, T. Torroba, C. F. Marcos, D. Miguel, J. Barbera, M. B. Ros and M. R. de la Fuente, *Chem.–Eur. J.*, 2005, **11**, 5362–5376.
- 16 M. Shimizu, M. Nata, K. Watanabe, T. Hiyama and S. Ujiie, *Mol. Cryst. Liq. Cryst.*, 2005, **441**, 237–241.
- 17 M. Shimizu, M. Nata, K. Mochida, T. Hiyama, S. Ujiie, M. Yoshio and T. Kato, *Angew. Chem., Int. Ed.*, 2007, **46**, 3055–3058.
- 18 H. Sato, K. Igarashi, Y. Yama, M. Ichihara, E. Itoh and K. Ohta, *J. Porphyrins Phthalocyanines*, 2012, **16**, 1148–1181.
- 19 K. Hatsusaka, K. Ohta, I. Yamamoto and H. Shirai, *J. Mater. Chem.*, 2001, **11**, 423–433.
- 20 L. Tauchi, T. Nakagaki, M. Shimizu, E. Itoh, M. Yasutake and K. Ohta, *J. Porphyrins Phthalocyanines*, 2013, **17**, 264–282.
- 21 J. F. van der Pol, E. Neeleman, J. C. van Miltenburg, J. W. Zwikker, R. J. M. Nolte and W. Drenth, *Macromolecules*, 1990, **23**, 155–162.
- 22 K. Ohta, T. Watanabe, S. Tanaka, T. Fujimoto, I. Yamamoto, P. Bassoul, N. Kucharczyk and J. Simon, *Liq. Cryst.*, 1991, **10**, 357–368.
- 23 M. Sorai and S. Seki, *Bull. Chem. Soc. Jpn.*, 1971, **44**, 2887.
- 24 M. Ichihara, A. Suzuki, K. Hatsusaka and K. Ohta, *J. Porphyrins Phthalocyanines*, 2007, **11**, 503–512.
- 25 K. Ohta, *Dimensionality and Hierarchy of Liquid Crystalline Phases: X-ray Structural Analysis of the Dimensional Assemblies*, Shinshu University Institutional Repository, submitted on 11 May, 2013, <http://hdl.handle.net/10091/17016>; K. Ohta, Identification of discotic mesophases by X-ray structure analysis, in *Introduction to Experiments in Liquid Crystal Science (Ekisho Kagaku Jikken Nyumon [in Japanese])*, ISBN-13: 978-4915666490, Japanese Liquid Crystal Society, Sigma Shuppan, Tokyo, 2007, ch. 2 and 3, pp. 11–21.
- 26 P. Herwig, C. W. Kayser, K. Müllen and H. W. Spiess, *Adv. Mater.*, 1996, **8**, 510–513.
- 27 S. Kumar, J. J. Naidu and D. S. S. Rao, *J. Mater. Chem.*, 2002, **12**, 1335–1341.
- 28 R. I. Gearba, M. Lehmann, J. Levin, D. A. Ivanov, M. H. J. Koch, J. Barberá, M. G. Debije, J. Piris and Y. H. Geerts, *Adv. Mater.*, 2003, **15**, 1614–1618.